Poly-Si(O)x passivating contacts for high-efficiency c-Si IBC solar cells

Yang, Guangtao; Zhang, Yue; Procel, Paul; Weeber, Arthur; Isabella, Olindo; Zeman, Miro

DOI
10.1016/j.egypro.2017.09.257

Publication date
2017

Document Version
Final published version

Published in
Energy Procedia

Available online at www.sciencedirect.com

ScienceDirect

Energy Procedia 124 (2017) 392–399

Energy Procedia

www.elsevier.com/locate/procedia

7th International Conference on Silicon Photovoltaics, SiliconPV 2017

Poly-Si(O)x passivating contacts for high-efficiency c-Si IBC solar cells

Guangtao Yang[1], Yue Zhang, Paul Procel, Arthur Weeber, Olindo Isabella, Miro Zeman

Delft University of Technology, Photovoltaic Materials and Devices group, Mekelweg 4, 2628 CD Delft, the Netherlands

Abstract

Highest conversion efficiency in crystalline silicon (c-Si) solar cells can be enabled by quenching minority carriers' recombination at c-Si/contact interface owing to carrier-selective passivating contacts. With the semi-insulating poly-crystalline silicon (SIPOS, poly-Si) a very good passivation of c-Si surfaces was obtained. We have explored these passivating structures on IBC solar cells and obtained over 22% efficiency with over 23% within reach on the short term. We present in detail the passivation quality of p-type and n-type ion-implanted LPCVD poly-crystalline silicon (poly-Si) and its relation to the doping profile. Optimized poly-Si layers in the role of emitter and BSF showed excellent passivation ($J_{0,emitter}$ = 11.5 fA/cm^2 and $J_{0,BSF}$ = 4.5 fA/cm^2) and have been deployed in FSF-based IBC c-Si solar cells using a simple self-aligned patterning process. Applying an optimized passivation of FSF by PECVD a-Si:H/SiNx layer ($J_{0,FSF}$ = 6.5 fA/cm^2) leads to a cell with efficiency of 22.1% (V_{OC} = 709 mV, J_{SC} = 40.7 mA/cm^2, FF = 76.6%). Since over 83% FF has been reached with adjusted metallization technology on similar IBC structures, we believe 23% efficiency is within reach on the short term. Further improvement, especially at J_{SC} level, is expected by deploying less absorbing carrier-selective passivating contacts based on poly-Si or wide bandgap poly-SiO_x layers (J_0 ~ 10 fA/cm^2).

Peer review by the scientific conference committee of SiliconPV 2017 under responsibility of PSE AG.

Keywords: poly-crystalline silicon oxide alloys; passivating contact; IBC c-Si solar cell;

1. Corresponding author. Tel.: +31 (0)15 27 86288; fax: +31 (0)15 27 82968
E-mail address: G.Yang@tudelft.nl

1876-6102
Peer review by the scientific conference committee of SiliconPV 2017 under responsibility of PSE AG.
10.1016/j.egypro.2017.09.257

1. Introduction

Highest conversion efficiency in crystalline silicon (c-Si) solar cells is enabled by quenching minority carriers' recombination velocity at c-Si/contact interface owing to carrier-selective passivating contacts [1]. The semi-insulating poly-crystalline silicon (SIPOS, poly-Si), with which very good passivation of c-Si surface was obtained [2], has recently attracted attention in several research groups as a high-temperature stable carrier selective contact [3,4,5]. Its structure comprises n-type or p-type doped poly-Si and tunnelling SiO_2 on c-Si wafer. With such structure high efficiencies were obtained both on front / rear contacted cells and interdigitated back contacted (IBC) cells [3,4,6,7].

In this work, optimized low sheet resistance, ion-implanted LPCVD poly-Si passivating contacts are discussed alongside their implementation into n-type bulk, FSF-based IBC solar cells. The passivation quality of such passivating contacts is found to be closely related to the doping profile at the poly-Si/c-Si interface; while the optimal thickness of tunneling SiO_2 is carried out directly at device level. A main drawback in using poly-Si layer is the higher parasitic absorption, mainly due to free carrier absorption. To reduce it, in-situ doped thin PECVD Si or SiO_x layers are optimized as passivating contacts to replace thick ion-implanted LPCVD poly-Si passivating contacts, aiming to improve the IBC cell efficiency from both the electrical and optical points of view.

2. Experimental

The process to make and the techniques to characterize symmetrical structures based on poly-Si passivating contacts and related IBC solar cells are described in this section. Our typical poly-Si passivating contact consists of an ultra-thin tunneling SiO_2 layer and a doped poly-Si layer, fabricated in a four-step process. First, the tunneling SiO_2 layer is formed on both sides of the wafer by a wet-chemical method; second, the intrinsic amorphous silicon (a-Si) is also deposited on both sides of the wafer by means of low-pressure chemical vapor deposition (LPCVD); third, an ex-situ single-sided doping process is realized using ion-implantation technique; fourth, a high temperature annealing step is carried out to activate and drive-in the implanted dopants while also turning the a-Si into poly-Si. In this work, <100> oriented, 1~5 Ωcm, 285-μm thick, double-side polished FZ wafers were used. The parameters used for the poly-Si passivating contacts preparation are listed in Table 1. The detailed descriptions of each step are presented in the following sub-sections.

The tunneling SiO_2 layer is formed by the method of Nitric Acid Oxidation of Silicon (NAOS). Before the NAOS process, in order to remove the native oxide, the Si wafer is dipped into HF, 0.55% for 4 min. The thickness of the obtained NAOS-based SiO_2 layer is ~1.5 nm (see Section IV.A). The a-Si layer is then deposited on the NAOS-based SiO_2 layer on both sides of the wafer by a Tempress LPCVD tube furnace at a temperature of 580 ºC. After the a-Si layer deposition, an annealing step at a temperature of 600 ºC for 1 hour is used to release the stress. In order to obtain a doped a-Si layer, a Varian Implanter E500HP is used to implant P or B atoms into the a-Si layer. With such an implanter, the implantation of B or P atoms can be done with a minimum energy of 5 keV and maximum dose of 10^{16} cm^{-2}. Therefore, the influence of the implantation parameters on the final passivation properties of poly-Si passivating contacts is studied. In this work, the P-implantation is done at fixed implantation energy of 20 keV and variable implantation dose; on the other hand, as the penetration depth of B is larger than P during the implantation, due to B atoms being smaller than P atoms, the B-implantation is done at lower fixed implantation energy of 5 keV and implantation dose of 5×10^{15} cm^{-2}. After the ion-implantation, a high temperature process is used to activate and drive-in the dopants. A Tempress tube furnace is used to anneal the samples in N_2 atmosphere. The annealing is here done at the temperature between 850 and 950 ºC. The ramping rate for heating or cooling is 10 ˚C/min. The effect of annealing time and atmosphere on the final passivation properties of poly-Si passivating contacts is also studied.

The injection-dependent minority carrier lifetime (τ) and implied open-circuit voltage (iV_{OC}) were measured by the Photoconductance Lifetime Tester (Sinton, WCT-120) using Quasi-Steady State Photoconductance (QSSPC) mode and transient mode. The values reported in this paper are taken from the transient analysis mode with an optical constant of 0.7 and at the minority carrier density of 1 x 10^{15} cm^{-3}. Four point probe measurement was used to obtain the sheet resistance (R_{SH}) of the passivating contacts. In order to ensure an accurate measurement, the c-Si bulk used for the R_{SH} measurement exhibited opposite doping type than the one of the passivating contacts under test.

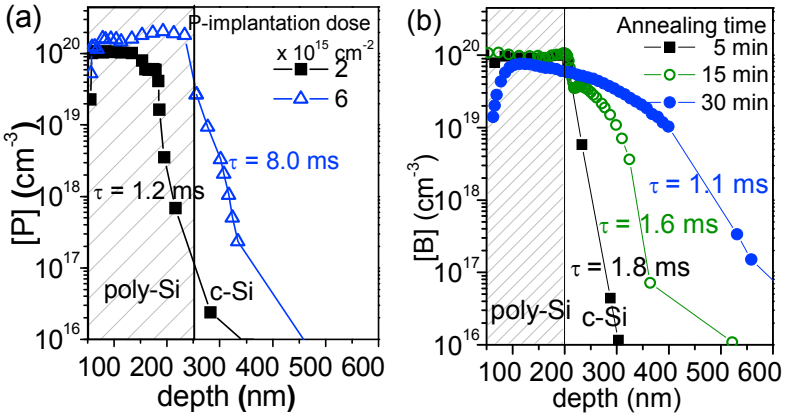

Fig. 1. (a) P-doping profile of 250-nm thick poly-Si passivating contacts (20 keV implantation energy and annealing at 950 ˚C for 5 min in N_2, but different implantation dose). (b) B-doping profile for 200-nm thick poly-Si passivating contacts (5 keV implantation energy, implantation dose of 5×10^{15} cm^{-2} and annealing at 950 ˚C in N_2 but different annealing time).

The IBC solar cell is processed with our self-aligned process flow [6,8]. It consists of P-implanted front surface field (FSF) on the front side, while the n^{++} doped poly-Si as BSF and p^{++} doped poly-Si as emitter are on the back side of the device. Due to the self-aligned process, there is always a gap, around 1-µm wide, between BSF and emitter, which will ensure no shunting between them. J-V curve of the IBC cells is measured with a AAA class Wacom WXS-156S solar simulator, while its series-resistance-free counterpart and its relative pFF are measured with a Sinton Suns-V_{OC}. The reference cells for both J-V and EQE measurements were calibrated at Fraunhofer Institute for Solar Energy Systems.

3. LPCVD poly-Si passivating contacts

The passivation quality of doped poly-Si is thought to depend on two aspects [9]: (i) the chemical passivation due to the tunneling SiO_2 layer and (ii) the field-effect passivation at the poly-Si/SiO_2/c-Si interfaces due to the dopants within the poly-Si layer. As the same NAOS process is used in all samples, the chemical passivation can be assumed to be equal among the samples. Thus, the variation in passivation properties obtained here is mainly attributed to the difference in the field-effect passivation.

Our results show that the symmetric sample with intrinsic poly-Si/SiO_2 layers has barely any passivation. Instead, when the ion-implanted P-dopants are mostly confined in the poly-Si material with a shallow profile in the c-Si bulk, a strong band bending is established at the poly-Si/c-Si interface, repelling the minority carriers from this interface. Therefore, a high field-effect passivation is obtained and a high minority carrier lifetime is observed, as seen in the sample with $6\times10^{15}cm^{-2}$ implantation dose in Fig. 1 (a). On the other hand, also in Fig. 1(a), no field-effect passivation occurs when the P-dopants are too shallow in the poly-Si material. Further, when the P-dopants

Table 1. Passivation properties of poly-Si(O)$_x$ passivating contacts on n-FZ wafer.

Sample	Bulk Si	Passivating contacts				Passivation		
		Deposition	Doping	Type	Thickness (nm)	Lifetime (ms)	J_0 (fA/cm^2)	iV_{OC} (mV)
1	n-FZ, flat	LPCVD	B-implantation	p-type poly-Si	250	5.4	11.5	716
2	n-FZ, flat	LPCVD	P-implantation	n-type poly-Si	250	15.0	4.5	733
3*	n-FZ, flat	PECVD	In-situ	p-type poly-SiO$_x$	35	2.1	25.0	692
4*	n-FZ, flat	PECVD	In-situ	n-type poly-Si	35	5.6	11.0	711
5*	n-FZ, textured	PECVD	In-situ	n-type poly-Si	30	4.1	8.5	717
6*	n-FZ, textured	PECVD	In-situ	n-type poly-SiO$_x$	35	4.9	12.0	710

* *For samples #3, #4, #5, #6: after the NAOS, in-situ doped PECVD a-SiO$_x$:H or a-Si:H layers are deposited on both sides of the wafer, followed by an annealing step at 850 ºC for 1 hour. Finally, before the lifetime measurement, the forming gas annealing (FGA) at 400 ºC for 2 hours is used for hydrogenation of the poly-Si(O$_x$) layer and its interface to the c-Si.*

diffuse too deeply in the c-Si bulk, there will be less or even no band bending on the c-Si side of the poly-Si/c-Si interface, resulting in a decrease of the passivation properties. As reported in Fig. 1(b), the passivating behaviour of B-implanted poly-Si passivating contacts shows similar trend as of P-implanted ones. When the B atoms are confined in the poly-Si material, a good passivation is observed, but when the B atoms diffuse too deeply into the c-Si bulk, passivation properties decrease. In particular, for different samples with the same poly-Si layer thickness, B-implantation parameters, and annealing temperature, but varied annealing time from 5 min to 30 min, B atoms diffuse deeper into the c-Si bulk for longer annealing, worsening the passivation. However, based on the simulation of tunneling and transport mechanisms, the doping tail within the c-Si bulk is necessary for an efficient carrier transport through the tunneling SiO_2 layer, which will eventually enhance the solar cell FF [10].

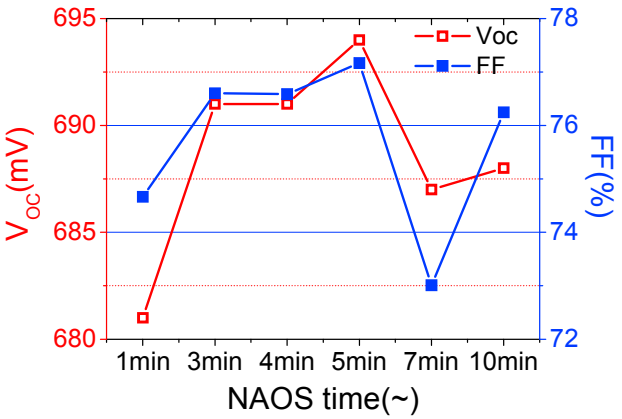

Fig. 2. V_{OC} and FF of fabricated IBC cells plotted against the single step NAOS-SiO_2 immersion time (69% HNO_3 bath at 110 ˚C).

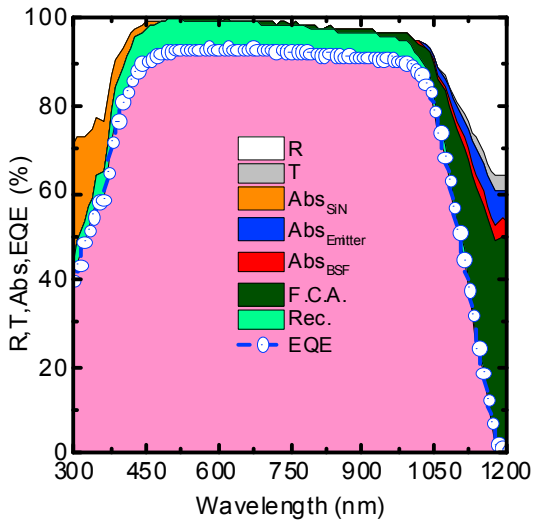

Fig. 3. The measured external quantum efficiency (EQE) of cell #4 (see Table 2), the reflectance (R) and transmittance (T) which are plotted as 1-R-T. The loss analysis is conducted by accurate TCAD Sentaurus optical-electrical simulator [10].

4. IBC solar cells with LPCVD poly-Si

Our IBC solar cells are endowed with an implanted FSF ($J_{0,front,text}$ = 192 fA/cm^2) on FZ n-type c-Si wafers. Emitter and BSF used in our cells are labelled, respectively, sample #1 and sample #2 in Table 1. Referring to

Table 2. Performance of IBC solar cells with different front side structure, passivation, and cell area.

Cell	Area (cm^2)	Metal thickness (μm)	FSF passivation	V_{OC} (mV)	J_{SC} (mA/cm^2)	FF (%)	pFF (%)	efficiency (%)
1	9.00	4	Thermal-SiO_2 / SiN_x	677	38.4	76.9	83.1	20.0
2	0.72	4	Thermal-SiO_2 / SiN_x	670	37.1	83.2	~	20.7
3	9.00	4	Thermal-SiO_2 / SiN_x	694	38.2	77.2	83.4	20.5
4	9.00	4 + 1.2	Thermal-SiO_2 / SiN_x	692	39.2	78.3	83.5	21.2
5	9.00	4	a-Si:H (5 nm) / SiN_x	705	37.8	69.7	72.4	18.6
6	0.72	4	a-Si:H (5 nm) / SiN_x	709	40.7	76.6	79.3	22.1
Target	9.00	> 4	a-Si:H (5 nm) / SiN_x	> 710	> 41.0	> 81.0	~	> 23.0

Table 2, in cell #1 a two-step NAOS was deployed to grow the tunneling SiO_2 layers. The first step is a 10-min long immersion in 99% HNO_3 at room temperature followed by rinsing in DI water; then, the second step is a 10-min long immersion in 68% HNO_3 at 110 ˚C, followed by rising in DI water and drying in N_2. With this two-step NAOS, cell #1 showed a V_{OC} of 677 mV and FF of 76.9%. As predicted by simulation [11], the cell FF is very sensitive to the thickness of the tunneling layer. Therefore we simplified our NAOS process by using only the abovementioned second step and we optimized it by varying the immersion time. Results at cell level reported in Fig. 2 show that the FF of the IBC cells indeed varies with the NAOS immersion time. The optimum immersion time was found to be 5 minutes, corresponding to a FF of 77.2%. Interestingly, also the V_{OC} of the cells correlates with the NAOS process and its maximum value (694 mV) was also measured from the cell with 5-min long NAOS immersion. Thus, based on optimal NAOS-SiO_2 tunneling layer, a cell efficiency of 20.5% was obtained (cell #3 in Table 1). As the lift-off process was deployed for metallization, metal fingers used at the back side of the IBC cell were limited to 4-μm thick e-beam evaporated Al. To examine the limitation of FF in cell #3, the metal fingers were covered again with 1.2-μm thick Al layer, leaving a 45-μm wide gap between BSF and emitter metal fingers (cell #4 in Table 1). This additional metallization increased further the FF to 78.3% (at almost constant pFF). That is, the FF of our cells is also limited by the metal finger conductivity, as confirmed by the FF of 83.2% obtained in cell #2, with an area of 0.72 cm^2. Due to higher metal coverage at the back side of cell #3, less light at longer wavelengths is lost in transmittance, increasing the cell J_{SC} to 39.2 mA/cm^2. This results in a final cell efficiency of 21.2%, measured without a reflecting chuck and illuminating the 3×3 cm^2 sized cell (including 2-mm wide bus bars).

The high $J_{0,front,text}$ of 192 fA/cm^2 limits however the solar cell V_{OC} and the carrier collection, as denoted in Fig. 3, where the EQE curve of cell #4 is reported, alongside measured reflectance (R), transmittance (T). The gap between the EQE and 1-R-T represents losses due to the parasitic absorption and the recombination losses, as accurately simulated by TCAD Sentaurus-based opto-electrical modelling [10]. It is found that the main losses come from the

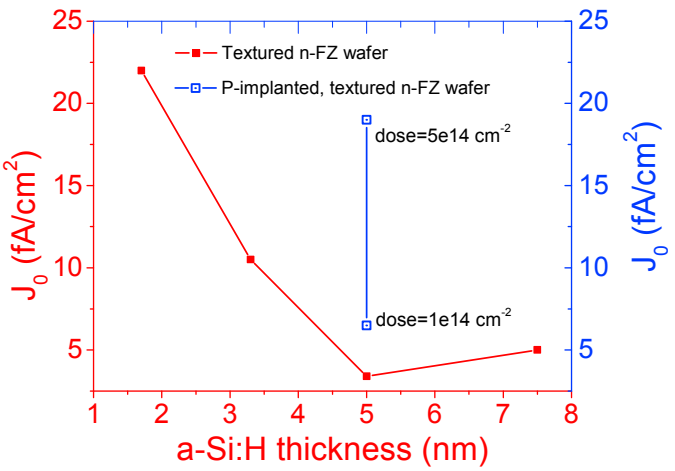

Fig. 4. Surface passivation quality (J_0) of P-ion implanted textured n-FZ wafers, which can be deployed as front side of the IBC solar cells, coated by PECVD a-Si:H/SiN_x stack as a function of the a-Si:H layer thickness and the doping level.

recombination, mainly from the FSF, and the parasitic absorption in the rear 250-nm thick poly-Si layers. To overcome these losses, from the electrical point of view, the FSF passivation is optimized; while from the optical point of view, more transparent novel passivating contacts are developed.

The FSF passivation is optimized with 5-nm thick of a-Si:H and 75-nm thick of SiN_x. The results are shown in Fig. 4. For textured but non-implanted wafer, a 1.7-nm thick a-Si:H coated by SiN_x layer is able to achieve a relatively high passivation (J_0 = 22.0 fA/cm^2). Increasing further the thickness of a-Si:H layer to 5 nm results in J_0 = 3.4 fA/cm^2. However, increasing the doping level of the textured wafer increases the J_0 from 6.5 fA/cm^2, in case of 10^{14} cm^{-2} implantation dose, to 19 fA/cm^2, in case of 5×10^{14} cm^{-2} implantation dose. For the solar cell process, the FSF implantation dose in IBC cells #5 and #6 is fixed at 10^{14} cm^{-2}, which is the same as cells #1 to #4, but passivated by 5 nm a-Si:H and 75 nm SiN_x layer. On the back side of these cells, 3-nm thick a-Si:H and 75-nm thick SiN_x layers are used to passivate the gap between BSF and emitter and to offer extra hydrogenation to the poly-Si

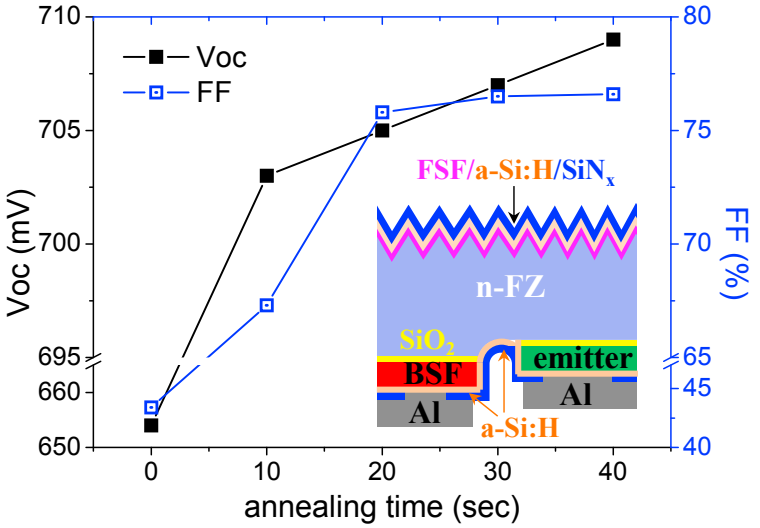

Fig. 5. The V_{OC} and FF of IBC solar cells with FSF passivated with a-Si:H/SiN_x as a function of annealing time at 600 ºC. Inset picture depicts cross sectional sketch of half pitch of IBC cell #5 and #6.The annealing is done step by step, with 10-second long steps.

layers. A cross-sectional sketch of the cell is shown as an inset in Fig. 5. The solar cell parameters are listed in Table 2. Due to the lower J_0 from the FSF, the higher V_{OC} of 709 mV for 0.72 cm^2 cell and 705 mV for 9 cm^2 solar cell are obtained after step annealing in N_2 environment for 40 sec at 600 ˚C with a step duration of 10 sec. The variation of V_{OC} and FF as a function of the step annealing time is shown in Fig. 5. The initial V_{OC} and FF are extremely low, 654 mV and 43.4%, respectively. However, the annealing treatment increases the V_{OC} and FF dramatically. The V_{OC} keeps on increasing until 709 mV after 40 sec annealing. We speculate that such increase is mainly attributed to two mechanisms: (1) The high temperature offers energy that drives the H atoms inside the a-Si:H layers and at the interfaces to the right position, where they passivate Si dangling bonds; (2) at high temperature, Al reacts with the a-Si:H layer on the rear side of the cell to form Al:Si alloy, which decreases the barrier between the Al contact and the BSF/emitter, thus lowering the contact resistance. However, the FF is saturated at around 76.5% after 20 sec annealing. Such low FF is due to shunting problems in the cells. This is proved by the low shunt resistance of 0.6 kΩ/cm^2 and low pFF_{max} of 79.3% for #6 (see Table 2). The I-V curve of this cell is shown in Fig. 6 as an inset; its slope in the low bias voltage range also indicates that there is shunt in the cell. The shunt path of the cell is attributed to the thin a-Si:H layer in the back side of the cell between the BSF and emitter

Thanks to the low J_0 of the FSF passivation, a better carrier collection is observed in cell #6, which induces a J_{SC} of 40.7 mA/cm^2, the EQE curve of this cell is shown in Fig. 6. Comparing to the EQE of cell #4, shown in Fig. 3, the recombination loss in cell #6 is minimized due to the high passivation quality of FSF in cell #6. However, some optical losses can still be pointed out as issues to tackle to further enhance the J_{SC}. Firstly, due to the not optimal

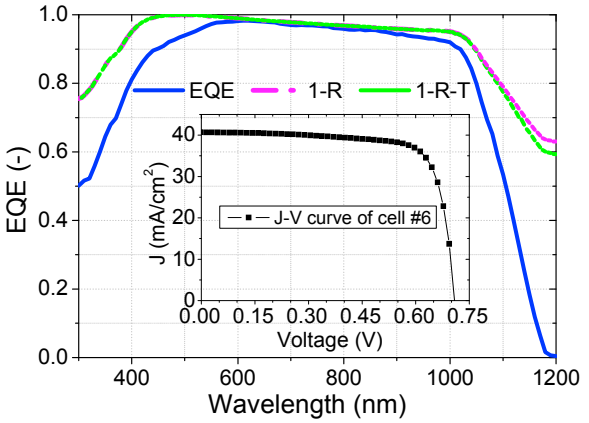

Fig. 6. EQE of cell #6 (see Table 2). Reflectance (R) and transmittance (T) are plotted as 1-R and 1-R-T.

anti-reflection on the front side of the cell, there is reflection loss in the long wavelength region, which can be seen from the high 1-R-T above 700 nm. Also in the short wavelength region, a parasitic absorption loss due to the a-Si:H/SiNx layer is noticeable. However, one of the main loss is the parasitic absorption in the 250-nm thick poly-Si BSF and emitter, due to their high free carrier absorption. The absorption coefficient of the n-type P-implanted LPCVD poly-Si passivating contract is shown in Fig. 7. The high doping in the poly-Si material causes a higher absorption coefficient in silicon at long wavelengths, which contributes to the loss in the EQE in the same wavelength region. In order to minimize this parasitic loss, the poly-Si layer can be made thinner. Therefore in-situ P-doped PECVD poly-Si (sample #4 and #5, in Table 1) are optimized and it is found that the n-type poly-Si exhibits much less absorbance than the P-implanted LPCVD poly-Si, mainly due to the lower doping. However, it has still an higher absorption coefficient than that of c-Si material. For further quenching the optical loss, we alloy the poly-Si with oxygen to open the bandgap of the poly-Si material, forming a poly-Si(O)$_x$ layer (sample #6, in Table 1). In the short wavelength region, all poly-Si(O)$_x$ materials exhibit higher absorption coefficient than c-Si, but much lower than a standard n-type a-Si:H. On the other hand, in the long wavelength region, once the poly-Si is alloyed with O, no absorption is recorded above 880 nm. By applying thin and doped PECVD poly-Si or poly-

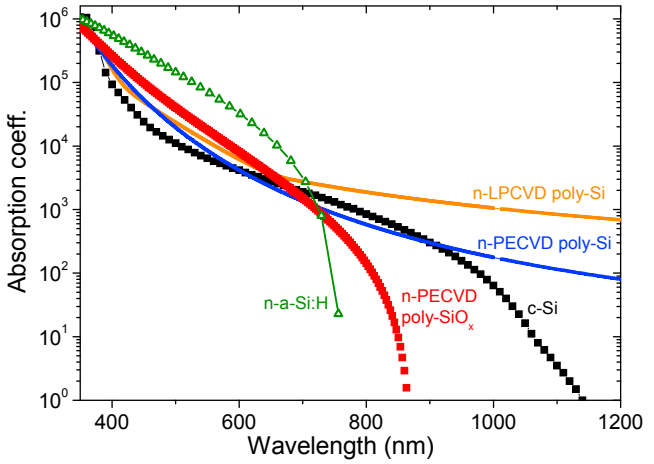

Fig. 7. Referring to samples in Table 1, absorption coefficient of the P-implanted LPCVD poly-Si (sample #2, orange curve), in-situ P-doped PECVD poly-Si (sample #4, blue curve), and in-situ P-doped poly-SiO$_x$:H (sample #6, red squares). The n-type a-Si:H (green triangles) and c-Si (black squares) curves are used here as references.

$Si(O)_x$ at the back side of the IBC cell, an extra gain in EQE in the long wavelength region is expected by minimizing parasitic absorption in both BSF and emitter and thus enhancing the J_{SC}.

5. Conclusions

Optimized ion-implanted LPCVD poly-Si with tunnelling SiO_2 passivating contacts applied in IBC solar cells are presented in this paper. The impact of doping profile at the poly-Si/c-Si interface of the passivating contacts on their passivation quality has been studied. Confining the implanted dopants within the poly-Si layer with a small in-diffusion tail into the c-Si bulk, an excellent surface passivation can be achieved. The V_{OC} and FF of the cells are found to be sensitive to the NAOS-SiO_2 tunnelling layer growth process. An a-Si:H/SiN_x stack minimizes the surface recombination related to P-implanted FSF, leading to a J_0 of 6.5 fA/cm^2 and inducing a V_{OC} as high as 709 mV by enhancing the carrier collection. The best IBC solar cell presents an efficiency of 22.1%, with V_{OC} = 709 mV, FF = 76.6%, and J_{SC} = 40.7 mA/cm^2. In order to further quench the optical losses, high passivation quality poly-$Si(O)_x$ layers are developed, which shows minimized absorption coefficient in the long wavelength region. By applying such poly-$Si(O)_x$ passivating contacts on the rear of the IBC solar cell, the cell J_{SC} will be further enhanced.

References

[1] Kaneka, Press release (14th Sept. 2016), http://www.kaneka.co.jp/kaneka-e/images/topics/1473811995/1473811995_101.pdf.
[2] Yablonovitch E, Gmitter T, Swanson RM, and Kwark YH, A 720 mV open circuit voltage SiO*x*/c-Si/SiO*x* double hetero-structure solar cell, Appl. Phys. Lett, 1985; 47:p.1211.
[3] Glunz SW, Feldmann F, Richter A, Bivour M, Reichel C, Steinkemper H, Benick J, Hermle M, The irresistible charm of a simple current flow pattern 25% with a solar cell featuring a full area back contact, 31st European Photovoltaic Solar Energy Conference and Exhibition, Hamburg; 2015.
[4] Römer U, Peibst R, Ohrdes T, Lim B, Krügener J, Wietler T, and Brendel R, Ion implantation for poly-Si passivated back-junction back-contacted solar cells, IEEE Journal of Photovoltaics, 2015; 5(2): p.507-514.
[5] Yan D, Cuevas A, Wan Y, Bullock J, Passivating contacts for silicon solar cells based on boron-diffused recrystallized amorphous silicon and thin dielectric interlayers, Solar Energy Materials and Solar Cells, 2016; 152:p.73-79.
[6] Yang G, Ingenito A, Isabella O, Zeman M, IBC c-Si solar cells based on ion-implanted poly-silicon passivating contacts, Sol. Energ. Mat. Sol, 2016; 15:p.884-90.
[7] Haase F, Kiefer F, Krügener J, Brendel R, Peibst R, IBC solar cells with polycrystalline on oxide (POLO) passivating contacts for both polarities, PVSEC-26, Singapore, 2016.
[8] Ingenito A, Isabella O, Zeman M, Simplified process for high efficiency, self-aligned IBC c-Si solar cells combining ion implantation and epitaxial growth: Design and fabrication, Sol. Energ. Mat. Sol, 2016; 157:p.273-279.
[9] Yang G, Ingenito A, Isabella O, Zeman M, Design and application of ion-implanted polySi passivating contacts for interdigitated back contact c-Si solar cells, Appl. Phys. Lett, 2016; 108:033903.
[10] P. Procel, G. Yang, F. Crupi, O. Isabella, M. Zeman, to be submitted, 2017.
[11] Steinkemper H, Feldmann F, Bivour M, and Hermle M, Numerical Simulation of Carrier-Selective Electron Contacts Featuring Tunnel Oxides, IEEE J. Photovolt., 2015; 5:p.1348-1356.